

QCD at DØ: A Review of Recent Results

Lee Sawyer

Louisiana Tech University, Ruston, LA 71272

Abstract. We report a variety of measurements of hadronic final states, ranging from elastic scattering of protons to events with highly energetic jets, based on data taken with the DØ experiment at the Fermilab Tevatron proton-antiproton collider.

Starting with the non-perturbative regime, we report measurement of the $p\bar{p}$ elastic differential scattering cross section, using DØ's Forward Proton Detectors (FPD). We present a new way to describe minimum bias events based on angular distributions in ≈ 5 million minimum bias $p\bar{p}$ collisions collected between April 2002 and February 2006 with the DØ detector. We demonstrate that the distribution of $\Delta\phi$ in the detector transverse plane between the leading track and all other tracks is a robust observable that can be used for tuning of multiple color interaction models. Pseudorapidity correlations of the $\Delta\phi$ distributions are also studied. In addition, we present a measurement of the effective cross section for events produced by double parton scattering.

DØ has produced a wide-variety of analyzes of final states involving jets, using a well-understood and calibrated data sample. Inclusive jet cross-sections, dijet production, and multi-jet production have been studied and compared to next-to-leading order (NLO) perturbative Quantum Chromodynamics (pQCD) predictions. After reviewing several published measurements, including the inclusive jet cross section and extraction of the strong coupling constant α_s , and the dijet angular dependence and azimuthal decorrelation, we present several recent analyzes. The differential inclusive dijet as a function of the dijet invariant mass M_{jj} , and the three-jet cross section as a function of the invariant three-jet mass ($M_{3\text{jet}}$), are measured in a data set corresponding to an integrated luminosity of 0.7 fb^{-1} . NLO pQCD calculations are found to be in a reasonable agreement with the measured cross sections.

Based on the same data set, we present the first measurement of ratios of multi-jet cross sections in $p\bar{p}$ collisions at $\sqrt{s} = 1.96 \text{ TeV}$ at the Fermilab Tevatron Collider. The ratio of inclusive trijet and dijet cross sections, $R_{3/2}$, has been measured as a function of the transverse jet momenta. The data are compared to QCD model predictions in different approximations.

Keywords: QCD, DØ, Tevatron, Jets

PACS: 12.38.Qk, 13.85.Hd

INTRODUCTION

In hadron-hadron collisions, production rates of collimated sprays of hadrons, called jets, are sensitive to both the dynamics of the fundamental interaction and to the partonic structure of the initial-state hadrons. The latter is usually parameterized in parton distribution functions (PDFs) of the hadrons. Thus measurements of jet production properties can be used to test the predictions of quantum chromodynamics (QCD) as well as to constrain the PDFs. Because jet production has the largest cross-section of any high p_T process at a hadron collider, the study of jet production provides the highest energy reach for the experiment and a unique sensitivity to new physics.

Several jet measurements are now well established at the Tevatron, including the measurement of the inclusive jet cross section and of the angular and invariant mass dependencies of dijet events. These measurements provide important tests of pQCD and

are input to PDF calculations. Measurements of multi-jet production take advantage of the fact that these processes have the same PDF sensitivity as dijet production, but are sensitive to processes to third order in the strong coupling constant α_s . Fundamental to the understanding of order α_s^3 processes is the three-jet cross-section, which we present as a function of the invariant mass of the three-jet system. Studies dedicated to the dynamics of the interaction are preferably based on observables which are insensitive to the PDFs. Such observables can be constructed as ratios of cross sections for which the PDF sensitivity cancels. In this note we report a measurement of $R_{3/2}$, the ratio of the inclusive three-jet to the inclusive 2-jet cross-sections.

While jet production is amenable to tests using perturbative QCD, there are many other processes at a hadron collider in which non-perturbative QCD predominates. It is also important to develop tests of the heuristic models that have been developed for non-perturbative processes, in order to compare them in detail to experimental results. To that end, we have developed a new analysis of angular correlation in tracks produced in so-called minimum bias events, using a sample of events constructed from secondary collisions in the same bunch crossing as an event with two high p_T muons. We have also studied events arising from double parton interactions, and made the first measurement of the $p\bar{p}$ elastic scattering cross section at $\sqrt{s} = 1.96$ TeV, employing detectors mounted in the far forward region of the DØ experiment.

THE DØ DETECTOR

The results presented in this paper are based on data taken with the DØ detector at the Fermi National Accelerator Laboratory's Tevatron $p\bar{p}$ collider. A detailed description of the DØ detector can be found in Ref. [1]. The event selection, jet reconstruction, jet energy and momentum correction in this measurement follow closely those used in our recent measurements of inclusive jet and dijet distributions [5, 6, 8]. The primary tool for jet detection is the finely segmented uranium-liquid argon calorimeter that has almost complete solid angle coverage $1.7^\circ < \theta < 178.3^\circ$ [1]. Jets are defined by the Run II midpoint cone jet algorithm [2] with a cone radius (for most jet studies) of $R_{\text{cone}} = \sqrt{(\Delta y)^2 + (\Delta\phi)^2} = 0.7$ in rapidity y and azimuthal angle ϕ . Rapidity is related to the polar scattering angle θ with respect to the beam axis by $y = 0.5 \ln[(1 + \beta \cos \theta)/(1 - \beta \cos \theta)]$ with $\beta = |\vec{p}|/E$. The jets in an event are ordered in descending transverse momentum p_T with respect to the beam axis.

The position of the $p\bar{p}$ interaction is reconstructed using a tracking system consisting of silicon microstrip detectors and scintillating fibers, located inside a 2T solenoidal magnet [1], and is required to be within 50 cm of the detector center along the beam direction. The jet four-momenta are corrected for the response of the calorimeter, the net energy flow through the jet cone, energy from event pile-up and multiple $p\bar{p}$ interactions, and for systematic shifts in y due to detector effects [5]. Cosmic ray backgrounds are suppressed by requirements on the missing transverse momentum in an event [5]. Requirements on characteristics of the shower shape are used to suppress the remaining background due to electrons, photons, and detector noise that mimic jets. The efficiency for these requirements is above 97.5%, and the fraction of background events is below 0.1% at all p_T^{max} .

ELASTIC SCATTERING AND MINIMUM BIAS EVENTS

A dedicated set of detectors placed near the beamline are used, in conjunction with the rest of the DØ detector and readout system, to study elastic and diffractive processes. These Forward Proton Detectors (FPDs) consist of eight quadrupole spectrometers, with six layers of scintillating fiber planes each. Data taken with the FPDs were produced under special running conditions of the Tevatron, characterized by single bunches and a $\beta^* = 1.6\text{m}$. An integrated luminosity of $\mathcal{L} \approx 30 \text{ nb}^{-1}$ was accumulated under these conditions.

In figure 1 the differential $p\bar{p}$ cross-section as a function of momentum transfer t , $d\sigma/d|t|$, is shown. The preliminary DØ measurement is indicated with black data points, and overlaid are previous results taken by the CDF[3] and E710[4] experiments at a $p\bar{p}$ cross-section of 1.8 TeV. our measurement extends the range of this measurement significantly, and provides the first measurement of the first diffraction minimum in the elastic differential cross section.

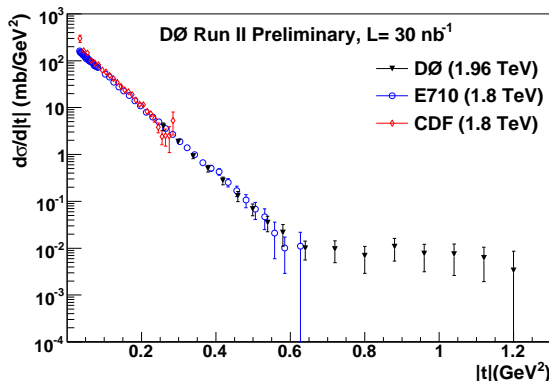


FIGURE 1. The preliminary DØ measurement of the $p\bar{p}$ elastic cross-section at 1.96 TeV, with comparisons to earlier measurements made at 1.8 TeV (see text for references).

While jet production is described reasonably well by perturbative QCD convoluted with PDFs, a variety of topics (usually grouped under the heading of “soft QCD processes”) are not amenable to a perturbative QCD calculation. These would include the development of showers in jets, the underlying events produced from the remnant partons of a collision and possibly initial state radiation, minimum bias events, etc. Models of these processes require comparison to experimental results in order to tune the model parameters. We have studied the angular separation in the detector transverse plane, $\Delta\phi$, between the leading track in the events ($p_{T\text{lead}}$ and all other tracks in the event, as a way to characterize minimum bias events. This variable is then compared to several Monte Carlo tunes and models.

In order to create a sample of minimum bias events, we first select events with exactly two muons with $p_T > 2 \text{ GeV}$, both associated with the primary vertex of the event. We require that the event contains one more additional minimum bias vertices, with at least five tracks associated to each vertex. These minimum bias vertices are required to be separated from the primary vertex by at least 5 cm, and to be within 20 cm of the center of the detector. All tracks are required to have $p_T > 0.5 \text{ GeV}$ and to be within $|\eta| < 2.0$.

Approximately 4.3 million minimum bias vertices were found to satisfy these selection requirements.

For each minimum bias vertex, the angular separation between the track with the largest p_T and every other track associated with the same minimum bias vertex is computed. The background-subtracted distribution (using a polynomial fit to the distribution) is then normalized to the number of tracks, as only the shape of the resulting distribution is important for comparison to models. The normalized, background-subtracted $\Delta\phi$ distribution is shown in Fig. 2, in bins of $\pi/50$, for two different ranges of leading track η .

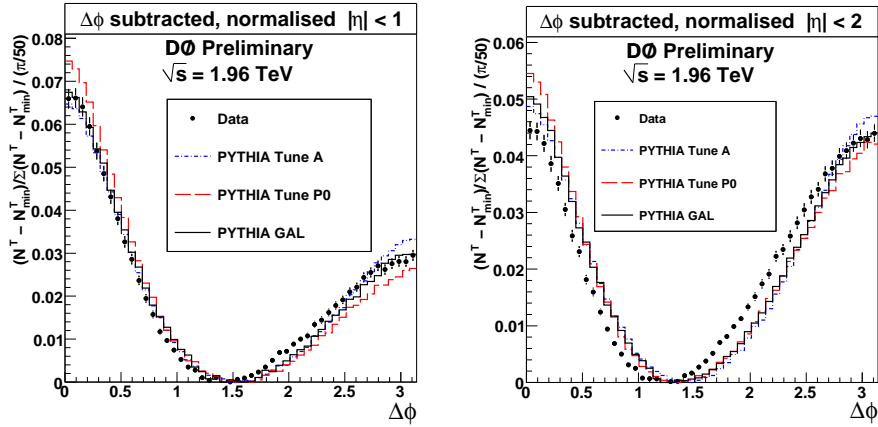


FIGURE 2. The normalized distribution of $\Delta\phi$ to the leading track in the same minimum bias vertex, for (a) $|\eta| < 1.0$ and (b) $|\eta| < 2.0$. Error bars include systematic uncertainties.

We have compared the distribution obtained from data with some tunes and models implemented in PYTHIA version 6.421 in two $|\eta|$ ranges: $|\eta| < 1$, historically the region for which tuning data is provided [20], and $|\eta| < 2$, the region accessible with the DØ detector. The comparison of the data $\Delta\phi$ distribution, subtracted and normalized, to three PYTHIA tune and model implementations (Rick Field’s Tune A [21], the Perugia 0 tune (P0) [22], and the Generalized Area Law model of color reconnections (GAL) [23]) in those two $|\eta|$ ranges are shown in Fig. 2 (a) and (b). These tunes and models were chosen because they have a range of interesting features. Tune A is historically significant and uses Q^2 -ordered parton showers, while tune P0 is a more recent tune which is an update of the First Sandhoff-Skands tune (S0) [28] and uses p_T -ordered showers. They both use the color-annealing model for color reconnections. GAL is based on tune S0 but uses the Generalized Area Law color reconnection model. In comparing the distributions in Fig. 2 (a) and (b), it is clear that the extended reach of the DØ detector allows us to access a region that affects the shape significantly and where the Monte Carlo tunes and models present large differences, increasing the tuning power.

We define a second observable by assigning the tracks to two η regions based on the rapidity of the leading track. We define tracks to belong to the “same” region if their η values have the same sign as the leading track, and “opposite” otherwise. We define our observable to be the distribution resulting from the subtraction of the “opposite” region distribution from the “same” region one, and then normalized, again minimizing the effect of fakes and tracking efficiency

The distribution of the “same-opposite” $\Delta\phi$ distribution is shown in Fig. 3, for the two ranges $|\eta| < 1.0$ and $|\eta| < 2.0$, along with the predictions from PYTHIA for the models listed before. Here the structure of the distribution broad and has a high same-side and flattened tail. The large η acceptance of the DØ detector allows us to access regions that affect the shape of this distribution, and where significant discrepancies between data and the Monte Carlo models exist.

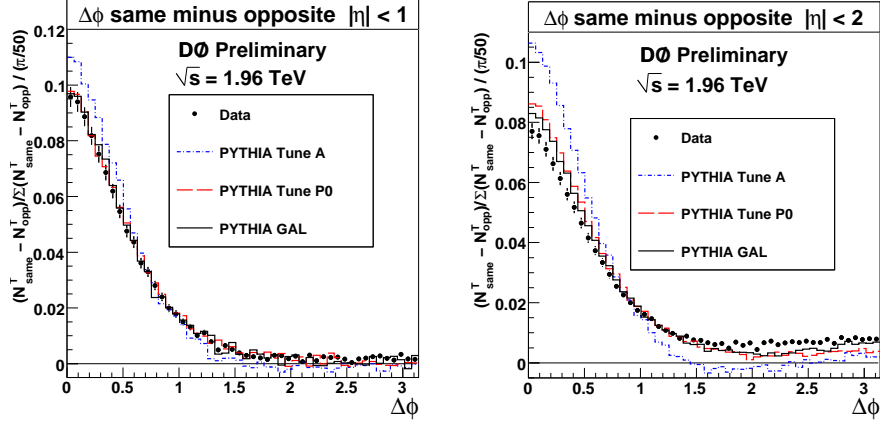


FIGURE 3. The normalized distribution of $\Delta\phi$ for same-opposite sides to the leading track in the same minimum bias vertex, for (a) $|\eta| < 1.0$ and (b) $|\eta| < 2.0$. Error bars include systematic uncertainties.

We evaluated the systematic uncertainties in our measurement by varying cuts in both data and Monte Carlo. The largest systematic uncertainty, approximately 1%, was found to be due to the minimum number of tracks required to construct a minimum bias primary vertex. The combined systematic uncertainties on both observables is estimated to be 2.8%.

Double Parton Events

Many features of high energy inelastic hadron collisions depend directly on the parton structure of hadrons. The inelastic scattering of nucleons need not to occur only through a single parton-parton interaction and the contribution from double parton (DP) collisions can be significant. The rate of events with multiple parton scattering depends on how the partons are spatially distributed within the nucleon. The DP cross sections can be expressed as [24][27] $\sigma_{DP} = \frac{\sigma_A \sigma_B}{\sigma_{eff}}$, where σ_A and σ_B are the cross sections of two independent partonic scatterings A and B. The process independent scaling parameter σ_{eff} has the units of cross section. Its relation to the spatial distribution of partons within the proton has been discussed in [24] through [27]. The ratio σ_B / σ_{eff} can be interpreted as the probability for partonic process B to occur provided that process A has already occurred.

We have measured the rate of DP events, using the data collected with the DØ detector during Run IIa, which after applying all the data quality criteria and the trigger selections, corresponds to an integrated luminosity of about $1.02 \pm 0.06 \text{ fb}^{-1}$. To determine the fraction of DP events, we select the sample of $\gamma + 3$ jets events with the require-

ment of only one event vertex (“1VTX” sample). The event vertex should have at least three associated tracks and the distance to the center of the detector along the beam axis should be less than 60 cm. There should be at least one photon candidate with p_T^γ between 60 and 80 GeV and passing quality cuts, and at least 3 jets with $p_T^{jet} > 25/15$ GeV (leading/second or third) and $|y| < 3.0$ and passing jet quality requirements.

The p_T spectrum for jets from dijet events falls faster than that for jets resulting from initial or final state radiation in the γ +jet events, and thus DP fractions should depend on the jet p_T [24][27]. The DP fractions and σ_{eff} are determined in three p_T^{jet2} bins 15–20, 20–25, and 25–30 GeV using a data driven method that exploits a difference in distributions of the ΔS variable; defined as $\Delta S = \Delta\phi(p_T^{\gamma,jeti}, p_T^{jetj,jetk})$, representing the opening angle of the two best balancing pairs of jets. The value of ΔS is chosen so that it minimizes on of the three variables $S_{p_T}, S_{p_T'}$, and S_ϕ , based on jet p_T resolution, average p_T , and ϕ resolution, respectively [29]. In most events, ΔS is minimized by pairing the photon with the leading jet.

In figure 4 we show the measured fraction of DP (f_{DP}) events, in three intervals of p_T^{jet2} . These are extracted from the $\Delta S_\phi, \Delta S_{p_T}$ and $\Delta S_{p_T'}$ as indicated in the figure. On the right, a comparison to the f_{DP} measurement is made to the PYTHIA Monte Carlo with two common tunes, tune A and Perugia tune S0 [28].

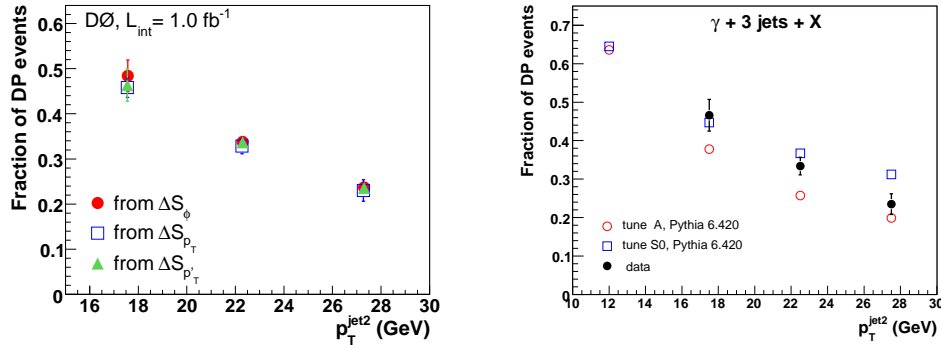


FIGURE 4. a) The fraction of double parton (DP) measured in three p_T^{jet2} intervals, extracted from the $\Delta S_\phi, \Delta S_{p_T}$ and $\Delta S_{p_T'}$ distributions described in the text. b) A comparison of the average measured fraction of DP events in the three p_T^{jet2} intervals, compared to prediction based on the PYTHIA Monte Carlo

The fraction of DP events, combined with a similar measurement of double interaction (DI) events, is used to extract the effective cross section σ_{eff} . Figure 5 shows the value of σ_{eff} measured in the three bins of p_T^{jet2} . Only a weak p_T dependence is observed. The value averaged over the three bins is $\sigma_{eff}^{ave} = 16.4 \pm 0.3(\text{stat}) \pm 2.3(\text{syst})$ mb.

INCLUSIVE AND DIJET PRODUCTION

The largest high p_T production cross section at a hadron collider is that of jets produced from final states containing quarks and/or gluons. This high cross section provides a unique sensitivity of new physics, but in the absence of new strong dynamics precision

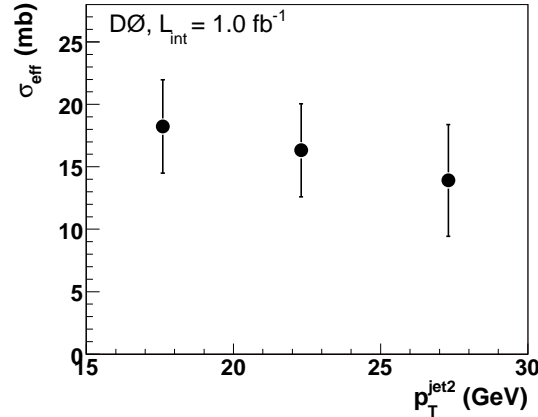


FIGURE 5. The effective cross section σ_{eff} for double parton (DP) events, as measured in three $p_T^{\text{jet}2}$ intervals.

jet measurements provide important tests of pQCD. The high reach of the Tevatron in both momentum transfer (Q^2) and parton momentum fraction x provides broad kinematic reach in which to test NLO pQCD predictions, as well as providing sensitivity to PDFs and the running of the strong coupling constant α_s .

For all jet studies, a jet energy scale (JES) correction is applied to jet four momentum as the measured four momentum of a jet is not the same as that of a jet entering the calorimeter due to the response of the calorimeter; energy showering in and out of the cone; and additional energy from detector noise, event pile-up and multiple $p\bar{p}$ interactions. The JES correction is determined using the p_T imbalance in γ + jet and dijet events. The additional energy from pile-up and multiple interaction is determined from a minimum bias sample. The JES corrections are of the order of 50% for a jet energy of 50 GeV and 20% for a jet energy of 400 GeV. However, for the 0.7 pb $^{-1}$ data sample used for the measurements presented in this talk, collected with the DØ detector during 2004–2005 in Run II of the Fermilab Tevatron Collider, the uncertainty on the JES is very small, less than 2% over jet p_T 's from 60 to 300 GeV.

For the sake of brevity, the reader is directed to reference [5] for a discussion of the inclusive jet cross section measurement, reference [9] for the details on the extraction of the strong coupling constant from the inclusive jet cross section, and to references [6] and [7] for discussion of the dijet chi and azimuthal decorrelation measurements.

More recently DØ has measured the dijet cross section as a function of the dijet invariant mass M_{jj} [8]. This cross section is measured in six regions of y_{max} , the rapidity of the leading jet in the event. Figure 6 (left) shows the resulting measurements, while figure 6 (right) shows the measured cross section divided by the NLO prediction from the NLOJET++ [10] program. This measurement is an important extension of pQCD to the forward region, and includes measurement of dijet invariant masses up to 1.2 TeV.

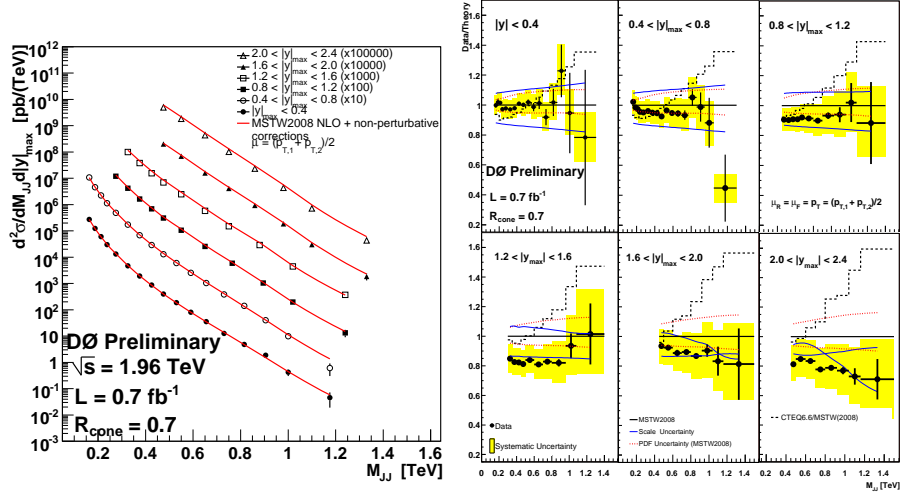


FIGURE 6. a) Dijet mass cross sections, shown for six regions of $|y_{max}|$. (Note that these regions scaled for plotting, with the exception of $|y_{max}| < 0.4$.) Full lines correspond to the NLO calculations with NLOJET++ and MSTW2008 PDFs. b) Dijet mass cross section divided by NLO prediction, with total systematic uncertainties indicated by the shaded bands. The dataset corresponds to an integrated luminosity of 0.7 fb^{-1} .

MULTIJET PRODUCTION

In the analyzes presented, we measured the trijet cross-section as a function of the invariant mass $M_{3\text{jet}}$ of the three-jet system, and study the ratio of the inclusive trijet and dijet cross sections.

In both the three-jet cross-section measurement and the measurement of $R_{3/2}$, events are triggered by a single high p_T jet above a particular threshold. In each p_T^{max} bin, events are taken from a single trigger which is chosen such that the trigger efficiency is above 99% for dijet and for trijet events. Jets in the $n = 2$ or 3 jet samples were selected with $|y| < 2.4$, and separation in the plane of rapidity and azimuthal angle, R_{jj} , between all pairs of the n leading p_T jets larger than twice the cone radius ($R_{jj} > 2 \cdot R_{\text{cone}}$). The rapidity requirement restricts the jet phase space to the region where jets are well-reconstructed in the DØ detector and the energy calibration is known to 1.2% – 2.5% for jets with $50 < p_T < 500 \text{ GeV}$. The separation requirement strongly reduces the phase space for which the n leading jets had overlapping cones which were split during the overlap treatment of the jet algorithm.

Measurement of $d\sigma/dM_{3\text{jet}}$ and $R_{3/2}$

We measure the differential inclusive three-jet cross section as a function of the invariant three-jet mass for three hard, well separated jets in three regions of jet rapidities ($|y| < 0.8$, $|y| < 1.6$, $|y| < 2.4$ for all three jets) and in three regions of the third jet transverse momentum ($p_{T3} > 40 \text{ GeV}$, $p_{T3} > 70 \text{ GeV}$ and $p_{T3} > 100 \text{ GeV}$) with leading

jet $p_T > 150$ GeV. The three-jet mass spectra are shown in Fig. 7.

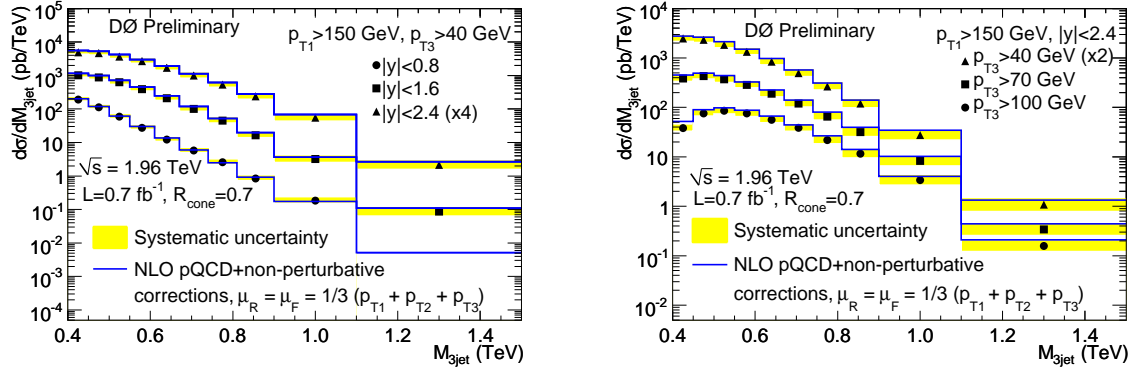


FIGURE 7. a) Three-jet mass cross section in regions of jet rapidities. The $|y| < 2.4$ region is scaled by a factor of 4 for readability. Systematic uncertainty is shown by shaded band. Full lines correspond to the NLO calculations with NLOJET++ and MSTW2008 PDFs. No events are found in the highest $M_{3\text{jet}}$ bin in $|y| < 0.8$ region. b) Three-jet mass cross section in regions of the third jet transverse momenta. The $p_{T3} > 40$ GeV region is scaled by a factor of 2 for readability. Systematic uncertainty in all three-jet mass bins is shown by shaded band. Full lines correspond to the NLO calculations with NLOJET++ and MSTW2008 PDFs. In both figures, the dataset corresponds to an integrated luminosity of 0.7 fb $^{-1}$.

The data are compared to the perturbative QCD NLO predictions calculated in NLOJET++[10] program with MSTW2008NLO[11] PDFs. The NLO prediction is corrected for hadronization and underlying event effects, with correction varied in the range from -3% to 6%, obtained from PYTHIA[12] simulations using tune QW[13]. The comparison of data to theory is shown in Fig. 8.

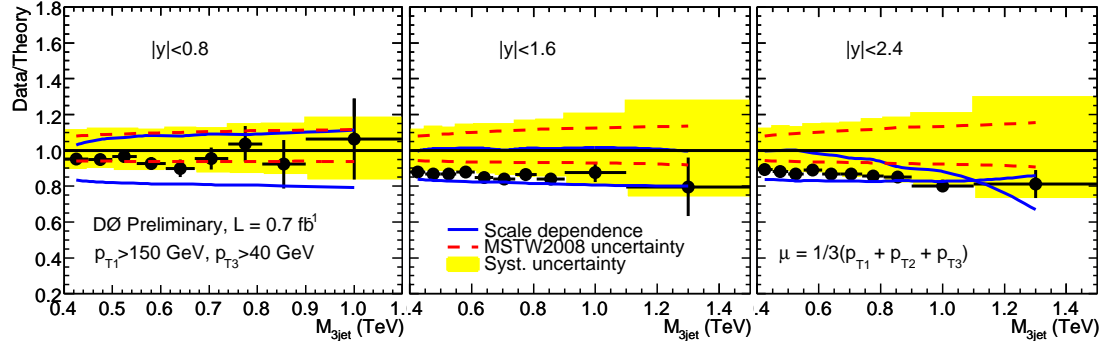


FIGURE 8. Data to theory ratio of the three-jet mass cross section in three regions of jet rapidities. The total systematic uncertainty is shown by a shaded band. The PDF uncertainty comes from the 20 MSTW2008NLO eigenvectors. The scale uncertainty is determined by varying the scale up and down by a factor of 2.

The ratio of inclusive jet cross sections, $R_{3/2}(p_T^{\text{max}}) = (d\sigma_{\geq 3\text{jet}}/dp_T^{\text{max}})/(d\sigma_{\geq 2\text{-jet}}/dp_T^{\text{max}})$, is less sensitive to experimental and theoretical uncertainties than the individual cross sections, due to cancellations of correlated uncertainties. Here $R_{3/2}$ is measured as a function of the leading jet p_T in an event, p_T^{max} , in the interval $(p_T^{\text{min}} + 30\text{GeV}) < p_T^{\text{max}} < 500\text{GeV}$, for p_T^{min} requirements of 50, 70, and 90 GeV.

The results are displayed in Fig. 9, where the inner error bars represent the statistical uncertainties while the total error bars represent the quadratic sums of statistical and systematic uncertainties. The data are compared to the predictions from different Monte Carlo event generators. The SHERPA v1.1.3 predictions [14], which include the tree-level matrix elements for 2-, 3-, and 4-jet production, are shown as solid lines in Figs. 9. These were obtained using default settings and MSTW2008LO PDFs and by matching the leading order matrix elements for 2-, 3-, and 4-jet production with a parton shower.

In addition, the data are compared to predictions from the PYTHIA event generator (version 6.422). The matrix elements implemented in PYTHIA are only those for 2-jet production. All additional jet emissions are produced by a parton shower. There are two different implementations, a virtuality-ordered parton shower and a p_T -ordered one. Both are highly tunable and more than 50 tunes are provided in PYTHIA v6.422. All tunes studies here use the CTEQ5L PDFs [15].

In Fig. 9 the data are compared to PYTHIA tunes which use the p_T -ordered parton shower [16, 17]. These are tune “Professor pT0” [18] and two extreme tunes from the “Perugia” series of tunes [19], the tunes “Perugia hard” and “Perugia soft”. All of these tunes give very different results for $R_{3/2}$ but all predict significantly higher ratios $R_{3/2}$ than what is seen in the data, even for the softest tune from the Perugia series.

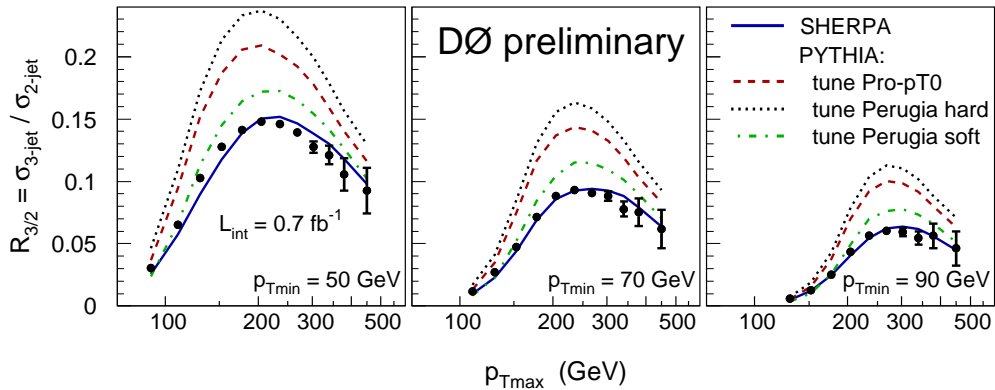


FIGURE 9. The ratio $R_{3/2}$ of trijet and dijet cross sections, measured as a function of the leading jet p_T (p_T^{\max}) for different p_T^{\min} requirements for the other jets. The predictions of SHERPA and PYTHIA (for three tunes using the p_T -ordered parton shower) are compared to the data.

SUMMARY

The $D\bar{O}$ experiment at the Fermilab Tevatron collider has been enormously successful, and continues to produce important physics measurements, tests of the Standard Model, and searches for new phenomena. Only a small portion of the QCD-related analyzes we have pursued could be shown in this talk. The reader is urged to check <http://www-d0.fnal.gov/results/index.html> for the latest results.

ACKNOWLEDGMENTS

This review represents the combined work of the many physicists and technicians working on the $D\bar{0}$ experiment. All credit for these results goes to this remarkable collaboration, while any errors in the reporting of these results are the author's own.

REFERENCES

1. V. M. Abazov *et al.* (D0 Collaboration), Nucl. Instrum. Methods Phys. Res. A **565**, 463 (2006).
2. G. C. Blazey *et al.*, in *Proceedings of the Workshop: QCD and Weak Boson Physics in Run II*, edited by U. Baur, R.K. Ellis, and D. Zeppenfeld, (Batavia, Illinois, 2000) p. 47, see Section 3.5.
3. F. Abe *et al.* (CDF Collaboration), Phys. Rev. D **50** 5518 (1994).
4. N. Amos *et al.* (E710 Collaboration), Phys. Lett. B **247** 127 (1990).
5. V. M. Abazov *et al.* (D0 Collaboration), Phys. Rev. Lett. **101**, 062001 (2008).
6. V. M. Abazov *et al.* (D0 Collaboration), Phys. Rev. Lett. **103**, 191803 (2009).
7. V. M. Abazov *et al.* (D0 Collaboration), Phys. Rev. Lett. **94**, 221801 (2005).
8. V. M. Abazov *et al.* (D0 Collaboration), Phys. Lett. B **693** 209 (2010). arXiv:1002.4594[hep-ex].
9. V. M. Abazov *et al.* (D0 Collaboration) Phys. Rev. D **80** 111107(R) (2009).
10. Z. Nagy, Phys. Rev. **D 68**, 094002 (2003); Z. Nagy, Phys. Rev. Lett. **88**, 122003 (2002).
11. A. D. Martin, W. J. Stirling, R. S. Thorne and G. Watt, Eur. Phys. J. C **63**, 189 (2009).
12. T. Sjöstrand *et al.*, Comput. Phys. Commun. **135**, 238 (2001).
13. M. G. Albrow *et al.* (TeV4LHC QCD Working Group), arXiv:hep-ph/0610012.
14. T. Gleisberg, S. Hoche, F. Krauss, M. Schonherr, S. Schumann, F. Siegert and J. Winter, JHEP **0902**, 007 (2009).
15. H. L. Lai *et al.* (CTEQ Collaboration), Eur. Phys. J. C **12**, 375 (2000).
16. T. Sjostrand and P. Z. Skands, Eur. Phys. J. C **39**, 129 (2005).
17. C. Buttar *et al.*, arXiv:hep-ph/0604120.
18. A. Buckley, H. Hoeth, H. Lacker, H. Schulz and E. von Seggern, arXiv:0906.0075[hep-ph].
19. P. Z. Skands, arXiv:0905.3418[hep-ph].
20. F. Abe, *et al.* (CDF Collaboration), Phys. Rev. Lett. **61**, 1819 (1988). F. Abe, *et al.* (CDF Collaboration), Phys. Rev. **D 41**, 2330 (1990).
21. R. D. Field (CDF Collaboration), in the *Proceedings of APS / DPF / DPB Summer Study on the Future of Particle Physics (Snowmass 2001)*, Snowmass, Colorado, 30 Jun - 21 Jul 2001, pp P501
22. P. Z. Skands, "The Perugia Tunes," (arXiv:hep-ph/0905.3418).
23. J. Rathsman, Phys. Lett. **B 452** (1999) 364
24. P. V. Landshoff and J. C. Polkinghorne, Phys. rev. D **18**, 3344 (1978).
25. C. Goebel, F. Halzen, and D. M. Scott, Phys. Rev. D **22**, 2789 (1980).
26. N. Paver and D. Trelani, Nuovo Cimento A **70**, 215 (1982); L. Ametlier, N. Paver, and D. Trelani, Phys Lett. B **169**, 289 (1986).
27. B. Humpert, Phys. Lett. B **131**, 461 (1983); B. Humpert and R. Odorico, Phys. Lett. B **154**, 211 (1985).
28. T. Sjostrand and P. Z. Skands, Eur. Phys. J. **C 39** (2005) 129
29. V. M. Abazov *et al.* (D0 Collaboration), Phys. Rev. D **81**, 052012 (2010).
30. W.K. Tung *et al.*, JHEP **0702**, 052 (2007).